International Journal of Architectural, Civil and Construction Sciences
ISSN: 2415-1734
Vol:13, No:10, 2019

Assessment of Pier Foundations for Onshore Wind Turbines in Non-cohesive Soil

Mauricio Terceros, Jann-Eike Saathoff, Martin Achmus

***Abstract*—**In non-cohesive soil, onshore wind turbines are often found on shallow foundations with a circular or octagonal shape. For the current generation of wind turbines, shallow foundations with very large breadths are required. The foundation support costs thus represent a considerable portion of the total construction costs. Therefore, an economic optimization of the type of foundation is highly desirable. A conceivable alternative foundation type would be a pier foundation, which combines the load transfer over the foundation area at the pier base with the transfer of horizontal loads over the shaft surface of the pier. The present study aims to evaluate the load-bearing behavior of a pier foundation based on comprehensive parametric studies. Thereby, three-dimensional numerical simulations of both pier and shallow foundations are developed. The evaluation of the results focuses on the rotational stiffnesses of the proposed soil-foundation systems. In the design, the initial rotational stiffness is decisive for consideration of natural frequencies, whereas the rotational secant stiffness for a maximum load is decisive for serviceability considerations. A systematic analysis of the results at different load levels shows that the application of the typical pier foundation is presumably limited to relatively small onshore wind turbines.

***Keywords*—**Onshore wind foundation, pier foundation, rotational stiffness of soil-foundation system, shallow foundation.

I. Introduction

ADVANCES in wind technology led to a considerable increase in the average capacity of Onshore Wind Turbines (OWT), resulting in the installation of large wind turbine generators founded on robust foundation supports. An optimization of geotechnical aspects of wind energy foundation is essential to obtain a cost-effective soil-foundation system, considering that the construction of infrastructure and foundation supports represents about 30% of the capital costs for wind energy projects, according to [8].

OWTs are commonly founded on shallow foundations (due to their simplicity) with a circular or octagonal shape as shown in Fig. 1 (a). The main characteristic of such foundation type is that the loads from the superstructure are transferred to the soil directly beneath the foundation by contact pressures in the base acting in the normal and tangential direction [1].

The shallow foundation consists of a massive reinforced concrete slab with large dimensions. The breadth of foundation ranges from 12 to 20 m with a circular pedestal of 5.5 to 6.5 m for the connection to the tower of OWT. The height of the foundation usually varies from 2 to 3 m, reducing towards the edges of the foundation. The depth of the foundation, which usually lies between 1 and 3 m, depends on the localization of the adequate load-bearing layers of soil as well as the minimum required depth to avoid damage caused by frost heave. Fig. 1 (a) shows a typically shallow foundation used for OWT.

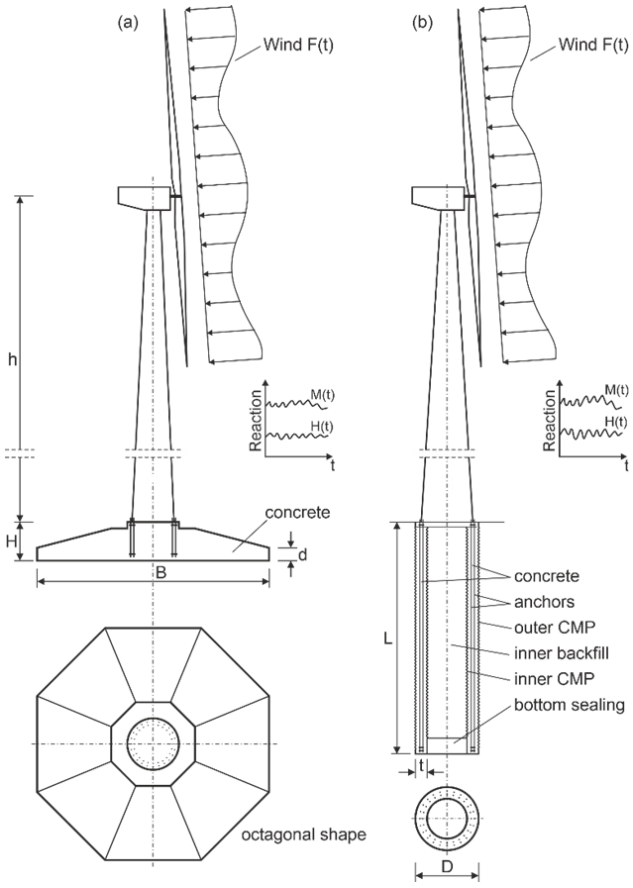

Fig. 1 Schematic sketch of shallow foundation (a) and pier foundation (b)

An alternative to shallow foundation might be a single pier foundation. An example for such a pier foundation is the "Patrick & Henderson (P&H)" tensionless pier foundation [6], which is schematically depicted in Fig. 1 (b). Consequently, a pier foundation has been considered to compare its load-

M. Terceros is with the Institute for Geotechnical Engineering, Leibniz Universität Hannover, 30167 Hannover (phone: 0049-511-7624153; fax: 0049-511-7625105; e-mail: terceros@igth.uni-hannover.de).
J.-E. Saathoff is with the Institute for Geotechnical Engineering, Leibniz Universität Hannover, 30167 Hannover (phone: 0049-511-7623808; fax: 0049-511-7625105; e-mail: saathoff@igth.uni-hannover.de).
M. Achmus is with the Institute for Geotechnical Engineering, Leibniz Universität Hannover, 30167 Hannover (phone: 0049-511-7624155; fax: 0049-511-7625105; e-mail: achmus@igth.uni-hannover.de).

bearing behavior with the typical support structure of OWT.

A particular characteristic of the pier foundation is that the head rotation may produce considerable resistance against the overturning moment by horizontal stresses acting between the pier shaft and the soil, according to [12].

The "tensionless pier foundation" depicted in Fig. 1 (b) is one of the foundation concepts, which have been used as foundation support OWTs. It was patented by Patrick & Henderson in the United States. The tensionless pier foundation consists of a reinforced concrete annular pier which is poured in situ between an internal and external corrugated metal pipe (CMP). In contrast to a conventional pier foundation, the entire length of the pier foundation remains in heavy axial compression by using a post-tension of steel anchors (hence the term "tensionless pier").

The mean diameter and length range from 4 to 5 m and 8 to 12 m, respectively. The ratio of the embedded tensionless pier length to diameter is usually set at around 2 to 4. The inner space is usually closed with a three-foot-thick lean concrete plug at the base, followed by un-compacted backfill material. Regarding the anchorage assembly, two circumferential rings of anchor bolts completely embedded in the concrete are held by a steel ring plate at the bottom of the pier. The anchor bolts that are projecting from the top of the foundation are post-tensioned by using the corresponding nuts, for further details see [19].

The foundations of the OWTs are subjected to dynamic and cyclic loading produced from the environmental conditions and the rotational effects of the rotor [2]. It is noted that the torsion and vertical loads are not decisive parameters to the design of wind turbine foundations since they are significantly smaller compared to the overturning moment and horizontal forces generated by highly eccentric loads.

In practical applications for OWT foundation system, the un- and reloading stiffness, which is relevant for the dynamic calculation, can be realistically approximated by the initial stiffness of the virgin load-deflection and moment-rotation curves, as described for monopile foundations in [13]. In this regard, the minimum rotational stiffness required for proper behaviour of the OWT under operation is one of the most important parameters provided by turbine manufacturers [11].

The present study aims to evaluate the technical and economic feasibility of the pier foundation based on a comprehensive parametric study which is used to evaluate the rotational stiffness of the novel soil-foundation systems. Thereby, three-dimensional numerical simulations of the pier and shallow foundations are developed using the program PLAXIS 3D [16]. A systematic comparison of the proposed foundation supports is undertaken in terms of the rotational stiffness at different load levels. Additionally, the behavior of the soil-pier system under un- and reloading is analyzed using a reference system with the traditional dimensions of the pier foundation to obtain correct predictions of the dynamical behavior being crucial for the eigenfrequency of the whole structure of OWT. It is assumed in all calculations that the groundwater level is below the bottom of the foundations, i.e. that no pore pressures occur in the soil.

II. State of the Art of the Geotechnical Design

The geotechnical limit state design for shallow foundations of OWT has to be fulfilled according to predefined conditions stated by numerous guidelines and recommendations such as [3] and [4]. For extreme loading events, the overall stability of the structure is guaranteed by the verification of Ultimate Limit State (ULS) design that includes base failure, resistance to overturning, open gap maximum to center gravity, and sliding proof. The Serviceability Limit State (SLS) design proves that the differential settlements and tilting are maintained within acceptable limits, also confirms the dynamic stiffness requirements and no open gaps under dead load conditions [14]. Finally, the Fatigue Limit State (FLS) design verifies that the soil-foundation system has sufficient stiffness to ensure that the eigenfrequencies of the overall structure remain within the acceptable limits to avoid resonance excitation resulting from the dynamic and cyclic loadings. In contrast, specific geotechnical design recommendations or design approaches for a pier foundation are quite limited. The experience from [7] is the most relevant reference for the design of the tensionless pier foundation. For the ULS proof, the overturning stability with a global safety factor of at least 2 has to be verified. The lateral head displacements ranging from 10 to 25 mm are stated as permissible. Regarding the SLS proof, a tilting under operational loads of maximal 1 mm/m and also lateral head displacements from 3 to 6 mm are allowed. In the FLS verification, rotational foundation stiffness has to be within the specified limits imposed by the respective OWT requirement to avoid resonance effects and excessive vibrations.

In this paper, translational and rotational stiffnesses are used to assess the behavior of the foundations. The secant stiffnesses ($K_{s,y}$ and $K_{s,\theta}$ respectively) of the soil-foundation systems under monotonic loading are derived from (1):

$$K_{s,y} = H / y \tag{1a}$$

$$K_{s,\theta} = M / \theta \tag{1b}$$

Herein, the ratio between the lateral force H and the lateral displacement y and also the overturning moment M and the rotation angle θ are described. For un- and reloading cycles, the procedure used remains unchanged, but the amplitude Δ of the evaluated cycle is considered, as shown in (2):

$$K_{s,y} = \Delta H / \Delta y \tag{2a}$$

$$K_{s,\theta} = \Delta M / \Delta \theta \tag{2b}$$

III. Numerical Simulation

A. General

The finite element program PLAXIS 3D was used to develop three-dimensional numerical models for the soil-foundation systems, whereby the respective foundation structure was subjected to axial and lateral loads in non-cohesive soil under consideration of various relative densities.

Due to the symmetry of both geometrical and load conditions, it suffices to model only one half of the foundation structure to reduce the computational effort. Preliminary analysis was also carried out to adjust the model dimensions, thus avoiding the influence of boundary effects on the behavior of the soil-foundation systems. Consequently, the breadth B of shallow foundations and the diameter D of the pier foundations were taken into account to normalize the model dimensions, resulting in widths of 8B and 21D in loading direction, lengths of 2B and 7D perpendicular to load direction, and model depths of 10H (height of foundation H) and 2L (length of pier L), respectively. The discretization of the model used in the numerical simulations amounts to an average of roughly 150000 elements (10-node tetrahedral), as shown in Figs. 2 and 3.

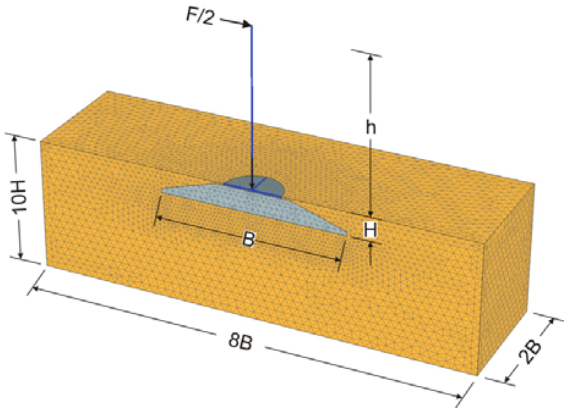

Fig. 2 Finite element mesh of the shallow foundation

Concerning the mesh fineness, local refinements were carried out in high-stress sectors such as at the base of shallow foundation as well as the soil surrounding the pier foundation. Likewise, artificial stress peaks at the corners of the triangular elements to model the cylindrical form are minimized.

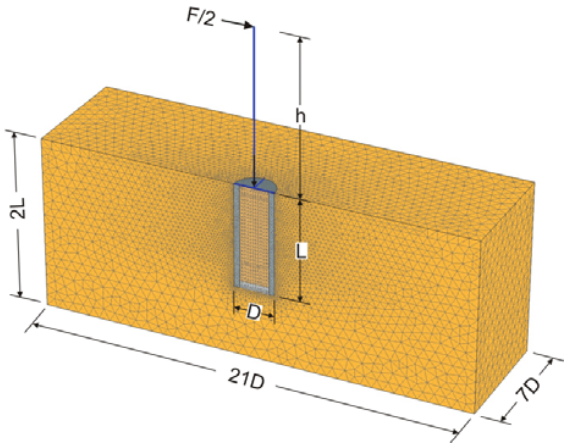

Fig. 3 Finite element mesh of the pier foundation

To ensure realistic conditions, a single vertical load that depends on the own weight of the OWT is directly applied in the center of the pedestal of the respective foundation support. Hereinafter, another single horizontal load is applied at the end of a rigid beam, which produces a significant moment loading due to the eccentricity of the load h.

Interface elements based on the bilinear Mohr-Coulomb material law were used to describe the interaction between the soil and the foundation supports (i.e., opening and sliding effects). The reduction factor R_{inter} in PLAXIS 3D to describe the concrete-soil interaction related to the strength of the interface with the soil was set to 0.8.

The foundation material (concrete, lean concrete, backfill material) is assumed to behave linear-elastic. The consideration of detailed modeling of the steel anchors is irrelevant here due to the exclusive examination of the external load-bearing behavior of the foundation supports. A concrete strength class C35/45 was considered for suitable modeling of the foundation. The material properties used for modeling of the foundation supports are listed in Table I.

TABLE I
APPLIED PARAMETERS FOR FOUNDATION MATERIALS

Description	Weight γ [kN/m^3]	Young's modulus E [MN/m^2]	Poisson's ratio ν, [-]
Reinforced concrete	25	34000	0.2
Lean concrete	23	10000	0.2
Backfill (Sand)	18	10	0.25
Rigid beam	0.1	1E10^9	-

The calculation for the numerical analysis was divided into four steps. In the first step, the initial stress state was calculated by the application of gravity loading with the application of the coefficient of horizontal earth pressure at rest k_0. In this step, only soil elements were taken into account. Afterwards, the examined foundation structures were installed in a "wished-in-place" procedure by the activation of the elements representing the foundation geometry as well as the contact between the foundation structure and the surrounding soil. The effects of foundation installation which might induce changes in the stiffness and strength properties of the soil around the foundation are clearly not considered, but such effects might be captured in practical design by empirical correlations, for instance. In the subsequent step, a vertical load (as own weight of OWT) was applied to the foundation structures. Finally, the foundation structures were subjected to lateral load with its respective moment (due to the eccentricity of the load).

B. Constitutive Law for the Soil

The Hardening Soil Model with small strain stiffness (HSsmall), according to [17], is used to model the soil behavior under virgin (monotonic) loading and un- and reloading cycles. This advanced model is an extension of the sophisticated Hardening Soil Model presented in [18], which applies a hyperbolic stress-strain relationship and a stress dependency of the soil stiffness. The HSsmall model takes into account increased stiffness at small strain levels, which is essential for dynamic applications and also for the determination of initial stiffnesses.

For very small shear strains, the soil stiffness can be described by the dynamic shear modulus G_0. An approach, according to [5], is used for the determination of G_0 in the proposed numerical model. This approach is valid for sandy soils with rounded grain. Such an empirical correlation of G_0 depends on the void ratio e, the power exponent λ_{G0}=0.5 and the mean principal stress σ'_m defined by the principal stress components σ'_1, σ'_2, σ'_3.

$$G_0 = 6900 \cdot \frac{(2.17 - e)^2}{1 + e} \cdot \sigma'^{\lambda_{G0}}_m \quad (3)$$

The degradation of the stiffness with shear strain is described by the following formulation proposed by [9].

$$G/G_0 = 1/\left(1 + (0.385 \cdot \gamma)/\gamma_{ref}\right) \quad (4)$$

The ratio between the current shear modulus G and the dynamic shear modulus G_0 depends on the value of shear strain γ, the reference shear strain $\gamma_{ref} = 10^{-4}$ and the shape factor a = 0.385. The reference shear strain γ_{ref} refers to the shear modulus G which is decayed to 72.2% of its initial value. For large shear strains, the degradation is limited by the static soil stiffness. The HSsmall material law distinguishes three moduli which are the secant stiffness in standard drained triaxial test E_{50}, the tangent stiffness for primary oedometric loading E_{oed} and the un- and reloading stiffness at engineering strains E_{ur}. All the total moduli in the HSsmall material law are based on a stress-dependent power-law controlled by an exponent m and a reference stress p_{ref}.

$$E_{oed} = E^{ref}_{oed} \cdot \left(\sigma'_1/p_{ref}\right)^m \quad (5)$$

$$E_{50} = E^{ref}_{50} \cdot \left(\sigma'_3/p_{ref}\right)^m \quad (6)$$

$$E_{ur} = E^{ref}_{ur} \cdot \left(\sigma'_3/p_{ref}\right)^m \quad (7)$$

$$G_0 = G^{ref}_0 \cdot \left(\sigma'_3/p_{ref}\right)^m \quad (8)$$

In this investigation, the dynamic shear modulus G_0 according to (8) is adjusted to (3). Similarly, the oedometric soil stiffness E_{oed} is adapted to the stress-dependent function based on the formulation proposed by [10] in (5). The stiffness parameter κ defines the soil stiffness at the reference stress σ_{at} = 100 kPa, and the exponent λ describes the stress dependency to the mean principal stress σ_m.

$$E_{oed} = \kappa \cdot \sigma_{at} \cdot (\sigma'_m/\sigma_{at})^{\lambda_{Eoed}} \quad (9)$$

The identical exponent m and the reference stress p_{ref} are used for the four moduli in PLAXIS 3D. These exponents of stress dependency, however, are often different for G_0 and E_{oed}, it is therefore required that the (homogeneous) soil is divided into several layers to adjust the stiffness profiles according to (3) and (9), respectively.

The moduli E_{50} and E_{ur} are defined as a function of the oedometric modulus E_{oed} as given in the linear equations (10) and (11):

$$E_{50} = (1 - \nu - 2 \cdot \nu^2)/(1 - \nu) \cdot E_{oed} \quad (10)$$

$$E_{ur} = 3 \cdot E_{50} \quad (11)$$

The soil parameters used for the simulations are introduced in Table II, depending on the relative soil density. The absence of groundwater was assumed in all cases.

TABLE II
SOIL PARAMETERS USED IN THE CALCULATIONS

Description		Unit	very dense	dense	medium dense
Void ratio	e	[-]	0.60	0.65	0.69
Unit weight	γ'	[kN/m^3]	20.3	20.0	19.75
Friction angle	φ'	[°]	40	37.5	35
Dilatancy	Ψ	[°]	10	7.5	5
Cohesion	c	[kN/m^2]	0.1	0.1	0.1
Poisson's ratio	ν	[-]	0.2	0.225	0.25
Stiffness parameter	κ	[-]	700	500	400
Stiffness parameter	λ_{Eod}	[-]	0.5	0.55	0.6
Stiffness parameter	λ_{G0}	[-]	0.5	0.5	0.5
Stiffness parameter	$\gamma_{0.7}$	[-]	0.0001	0.0001	0.0001

C. Validation of the Numerical Model

The authors do not have access to field tests of pier foundations with detailed documentation that could be used to validate the results of the sophisticated three-dimensional numerical models. The calibration of the systems is mainly based on the experience of authors. Indeed, the validation of the results by field measurements is highly recommended for the readjustments of numerical simulations. However, based on the fact that the comparative study is mainly carried out between two types of foundations that use the identical advanced material law HSsmall, the results are assumed to be valid as a reference of the load-bearing behavior of the foundation supports examined.

IV. Results for a Reference System

A typical pier foundation [19], as it is often used in onshore wind farms in the United States, has been selected as a reference system. It has a length L = 12 m with a mean diameter D_m = 4 m. The constant wall thickness over the depth amounts to t = 0.65 m. The lateral load is applied with eccentricity h = 60 m as the type of wind turbine N80/2500 R60 (see Table III). The pier is embedded in homogeneous very dense sand. The soil parameters listed in Table II were applied.

For comparison of load-bearing behavior under different load conditions, a purely virgin (monotonic) loading and also five intermediate un- and reloading cycles were applied separately in the introduced reference system. Firstly, a vertical compressive load of 3000 kN which corresponds to the own weight of the OWT was applied. Subsequently, the lateral load steps are increased until the pier head rotation of 1.0 mm/m is reached, which is a reference for tilting under

operational load according to [7].

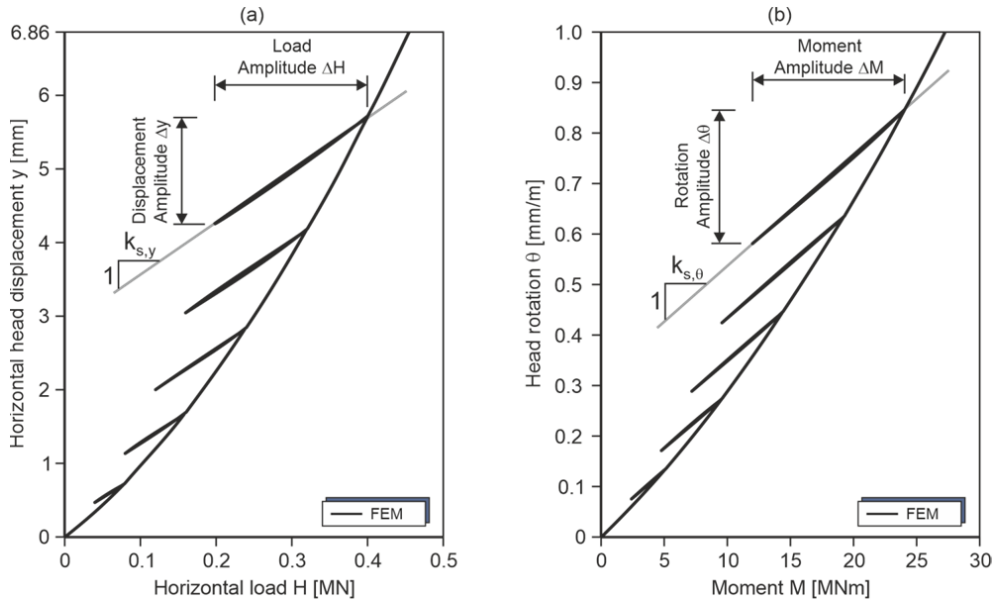

Fig. 4 Pier foundation reference system: Numerically calculated load-deflection (a) and moment-rotation (b) curves for cyclic loading with 50% cyclic load span

In Fig. 4, the results of the examined reference system with the application of virgin (monotonic) loading and un- and reloading cycles are provided in terms of load-deflection and moment-rotation curves. An un- and reloading span of 50% of the previously applied load is considered to reproduce un- and reloading cycles. The un- and reloading stiffnesses are represented by translational and rotational stiffness ($K_{s,y}$, $K_{s,\theta}$) for the related un- and reloading cycles.

To complete the analysis, Fig. 5 shows the comparison of the load-bearing behavior in terms of secant stiffness for the virgin loading and also the un- and reloading cycles with different spans. Four simulation series were conducted with un- and reloading load spans of 25%, 50%, 75% and 100% of the previously applied maximum load to obtain a clear appreciation of the un- and reloading stiffness of the soil-foundation system.

Evidently, the secant stiffnesses for the un- and reloading spans are considerably larger than the secant stiffnesses of the virgin (monotonic) loading for operational loads. The smaller un- and reload spans compared to the virgin loading yield larger deviations than 100% full unloading span. Additionally, Fig. 5 (b) shows the rotation values θ of 0.001, 0.2, 0.5 and 1.0 mm/m which are examined in the parametric study carried out in Section V.

The variation of the secant stiffness for the different un- and reloading spans is rather small. Independent of the considered load span, the secant stiffness is almost equal to the initial stiffness of the virgin loading curve. This justifies the usual approach in practical design to use the initial stiffness in the calculation of eigenfrequency. The initial slope of the translational secant stiffness $K_{y,0}$ and also the rotational secant stiffness $K_{\theta,0}$ shown in Fig. 5 are represented by gray lines.

V. Parametric Study

A. General Procedure

A comprehensive parameter study is carried out using 3D finite element models for the pier and the shallow foundation. The load-bearing behaviors are thoroughly examined to compare both types of foundations. For such purpose, the foundation geometries, the soil properties, and the load conditions are varied.

For the geometry of shallow foundation, the breadth (or equivalent diameter) ranges from 12 to 24 m. The depth of the footing d is varied as a function of the breadth B. Concerning the pier foundation, three predefined diameters (D_m = 4, 5, 6 m) with the respective wall thicknesses (t = 0.65, 0.75, 0.85 m) and the load eccentricities (h = 60, 91, 120 m, depending on the type of OWT) were examined. In the analysis, the pier length L was varied in a range from 9 to 21 m. It is noted that the geometry of the reference system is integrated into the parametric study with the aim to facilitate comparison. The geometrical parameters used for the simulations are collected in Table IV.

The presented study is limited to homogeneous non-cohesive soil profiles with relative densities for very dense, dense, and medium dense state.

Concerning the load conditions, three types of wind turbines are considered, each one with specified characteristics with regard to their own weight and hub height. A summary of the load conditions is given in Table III.

Initially, an axial load (own weight) was applied based on the type of OWT. Subsequently, the horizontal load steps were increased to a maximum head rotation of 5 mm/m to achieve a wide range of load levels.

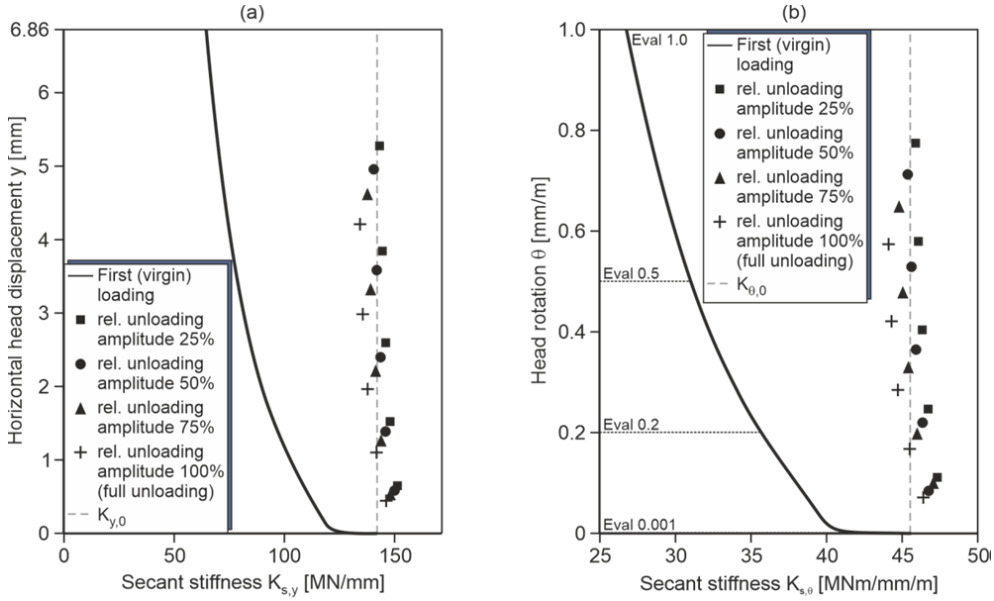

Fig. 5 Pier foundation reference system: Translational (a) and rotational (b) secant stiffness for monotonic and cyclic load spans for different relative levels of unloading

Seven head rotations of foundation support θ = 0001, 0.2, 0.5, 1, 2, 3, 4, and 5 mm/m were selected to display the degree of non-linearity of the soil-behavior at different load levels. The eccentricity of the horizontal load depends on the hub height of the OWT.

The initial stiffness defined at 0.001 mm/m is within the spectrum of loads, considering as a crucial parameter for the un- and reloading stiffness as introduced in Section IV.

TABLE III
LOAD CONDITIONS ACCORDING TO TYPE OF OWT

Description	Axial load l_A [kN]	Rotation θ [mm/m]	Hub height h [m]
N80/2500 R60	3000	5.0	60
N117/3000 R91	5000	5.0	91
N117/3000 R120	8000	5.0	120

Technical data of OWTs have been selected with reference to [15].

The numerical results are given in terms of rotational secant stiffness $K_{s,\theta}$, depending on the breadth B of footing and the pier length L shown separately in Figs. 6 and 7. A total of 180 foundation-soil systems were investigated to reproduce the curve diagrams and to evaluate the behaviors of the soil-foundation systems with the predefined head rotations.

Fig. 8 shows the results of a comparison study which was subsequently conducted based on the dimensions of the structure supports, whereby the load transfer mechanisms were considered decisive for the selection of the most relevant variables of both foundation supports. The pier foundation transfers mainly the horizontal loads to the soil by the shaft surface being, in this case, the pier length decisive for the bearing capacity. Instead, the breadth at the base (used to calculate the contact area) turns out to be relevant for the load transfer of the shallow foundation. Therefore, the embedded length of the pier L and the breadth of the footing B are compared for three predefined head rotations θ = 0.001, 1, and 3 mm/m.

The procedure used for the comparison consists of the identification of the rotational secant stiffness that coincides for both foundation supports in the respective predefined head rotations. i.e., each curve represents a head rotation whereby the rotational secant stiffness is identical for both corresponding foundation types. The three predefined diameters of the pier foundation were used with their respective characteristics to reach the rotational stiffness of the shallow foundation in the entire range of breadths.

TABLE IV
SOIL PARAMETERS USED IN THE CALCULATIONS

Pier foundation				Shallow foundation			Load Ecc.
D_m[a] [m]	L [m]	L/D_m [m]	t [m]	B [m]	H [m]	d [m]	h [m]
4.0	9.0	2.25	0.65	12	1.95	0.35	60/91/120
4.0	12.0	3.0	0.65	15	2.20	0.4	60/91/120
4.0	15.0	3.75	0.65	18	2.45	0.45	60/91/120
4.0	18.0	4.50	0.65	21	2.7	0.5	60/91/120
4.0	21.0	5.25	0.65	24	2.95	0.55	60/91/120
5.0	9.0	1.8	0.75				60/91/120
5.0	12.0	2.4	0.75				60/91/120
5.0	15.0	3.0	0.75				60/91/120
5.0	18.0	3.6	0.75				60/91/120
5.0	21.0	4.2	0.75				60/91/120
6.0	9.0	1.5	0.85				60/91/120
6.0	12.0	2.0	0.85				60/91/120
6.0	15.0	2.5	0.85				60/91/120
6.0	18.0	3.0	0.85				60/91/120
6.0	21.0	3.5	0.85				60/91/120

[a] The designations of the respective foundation geometries are described in detail in Fig. 1. D_m = mean diameter.

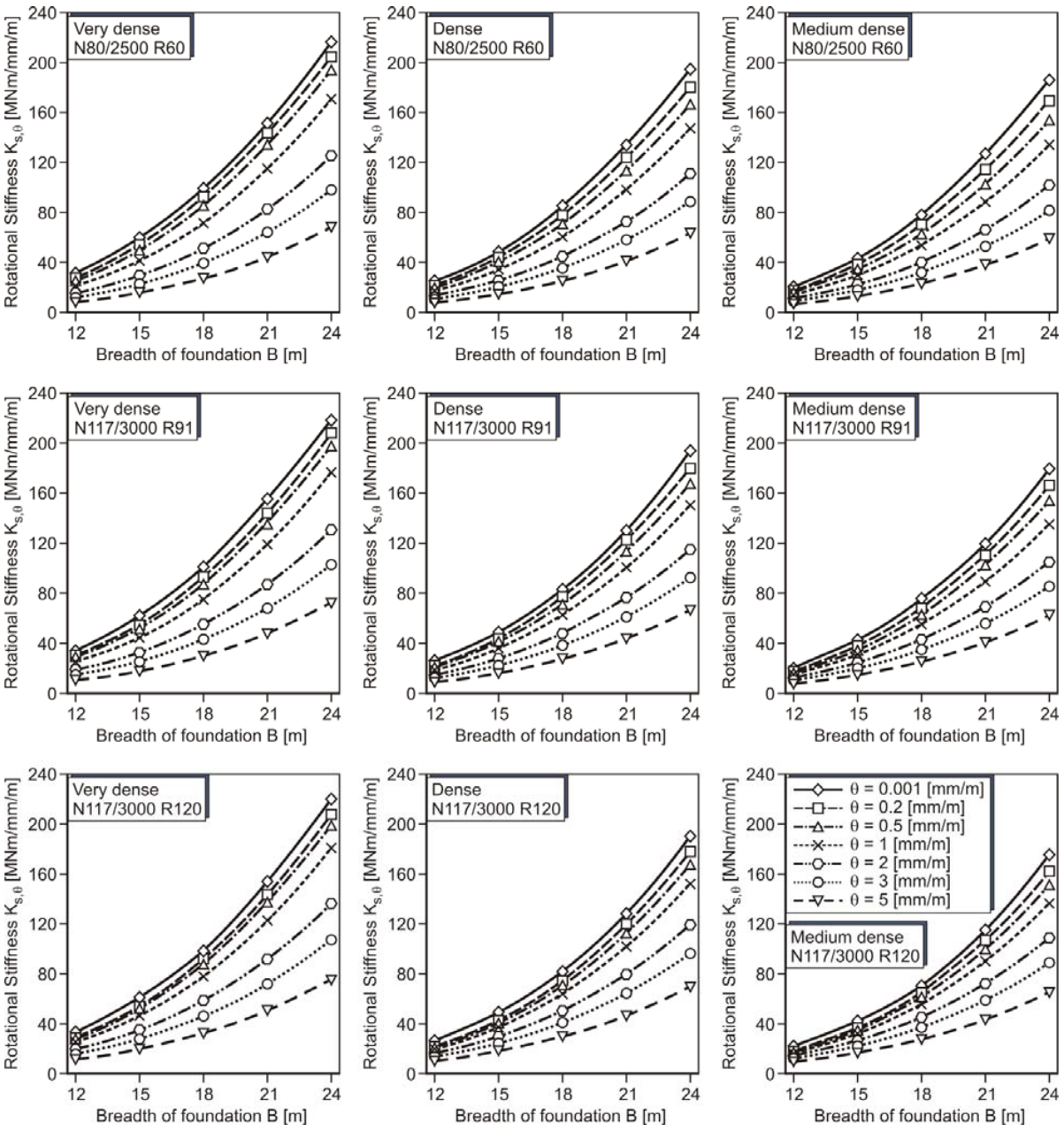

Fig. 6 Shallow foundation: Influence of the foundation breadth on the rotational secant stiffness

B. Results of the Parametric Study

Fig. 6 shows the rotational secant stiffness of shallow foundations as a function of the breadth for seven pre-defined head rotations. The trend lines produced by the ascending rotational stiffness with the increasing breadth are quite different from the lines generated for pier foundations (Fig. 7).

The main difference is that the rotational stiffness of the shallow foundation would not reach a constant value with enlarged breadth as the pier foundation does.

In addition to the variation of the breadth, the load conditions were adjusted according to the type of OWT given in Table III. Concretely, the axial loads due to their own weight and also the eccentricity of lateral loads (hub height) varied.

Very similar results were expected between the soil-foundation systems with the different types of OWT since the rotational stiffnesses are determined by the ratio between the overturning moment M and the rotation angle θ. In other words, the rotational stiffness is not directly impacted by the load eccentricity. Nonetheless, a slight difference is observed due to the variation of the axial loads, which depends on the type of wind turbine structures.

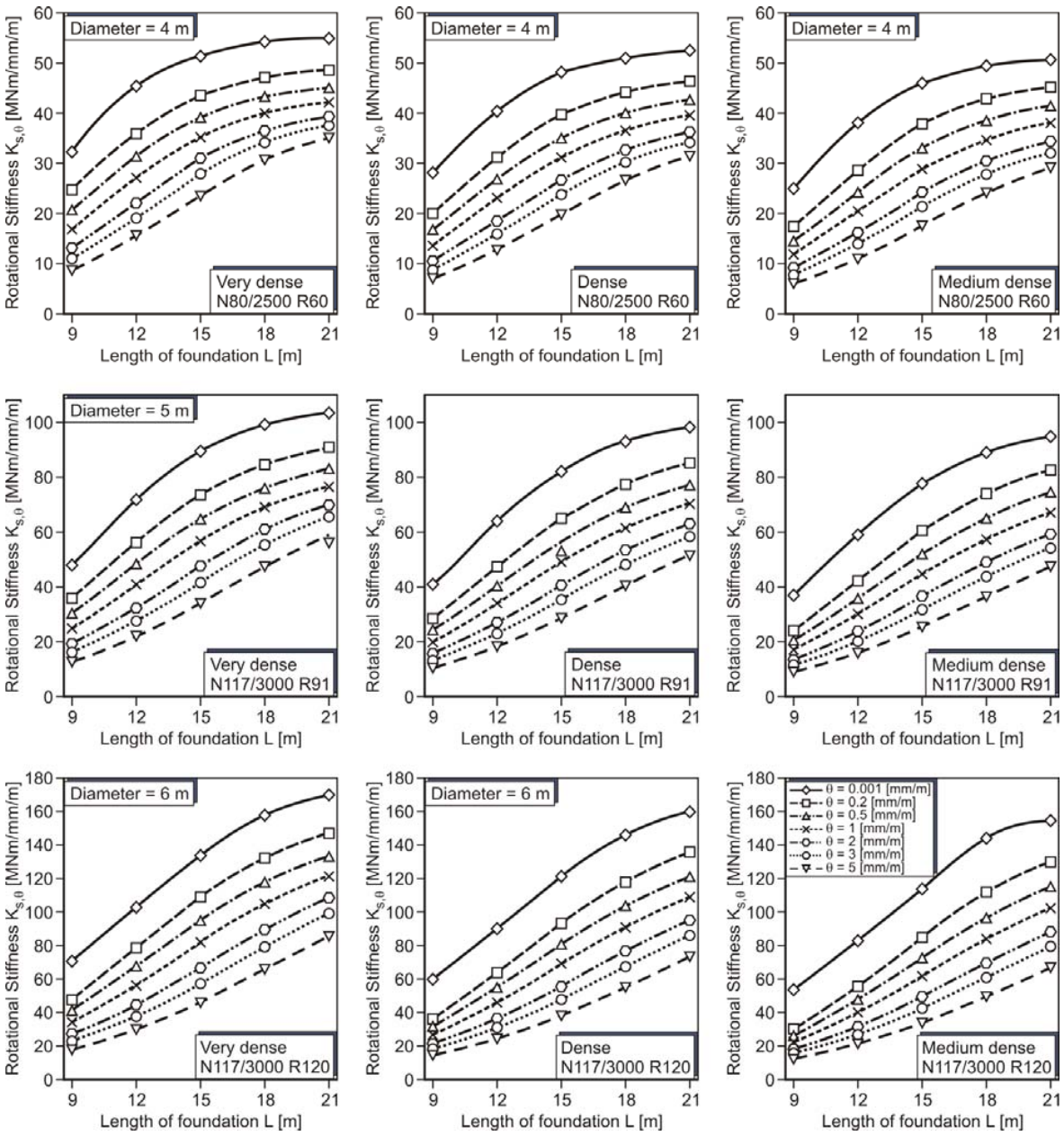

Fig. 7 Pier foundation: Influence of the foundation length on the rotational secant stiffness for three predefined diameters (4, 5, 6 m)

In Fig. 7 the rotational secant stiffness of the pier foundation is depicted for seven pier head rotations, too. Three diameters of the pier foundation are considered, whereby the geometry and load conditions are adapted (see Table IV).

The increased pier length yields an increase of the rotational secant stiffness. Nevertheless, the rotational stiffness ceases to increase when a critical pier length is reached. This can be explained by a flexible behavior produced by the long pier foundations. An identical behavior is observed at horizontally loaded pile foundations. It is also noted that for the smallest pier head rotation $\theta = 0.001$ mm/m the non-linearity of the behavior is more pronounced than for other head rotations. This effect is probably caused by the strain-dependence of stiffness introduced by the sophisticated material law HSsmall.

Finally, the effect of a variation of pier diameter is evident. An increasing diameter leads to a considerable increment of the rotational secant stiffness (between 30 to 50% per meter increase).

Fig. 8 provides a correlation between the pier lengths L and the breadths B of footing. Using the rotational secant stiffness illustrated in Figs. 6 and 7, the equivalent dimensions are determined for three predefined head rotations. It is noteworthy that both types of foundations are compared under identical load and soil conditions. A marked nonlinearity is visible in the correlation of all predefined head rotations.

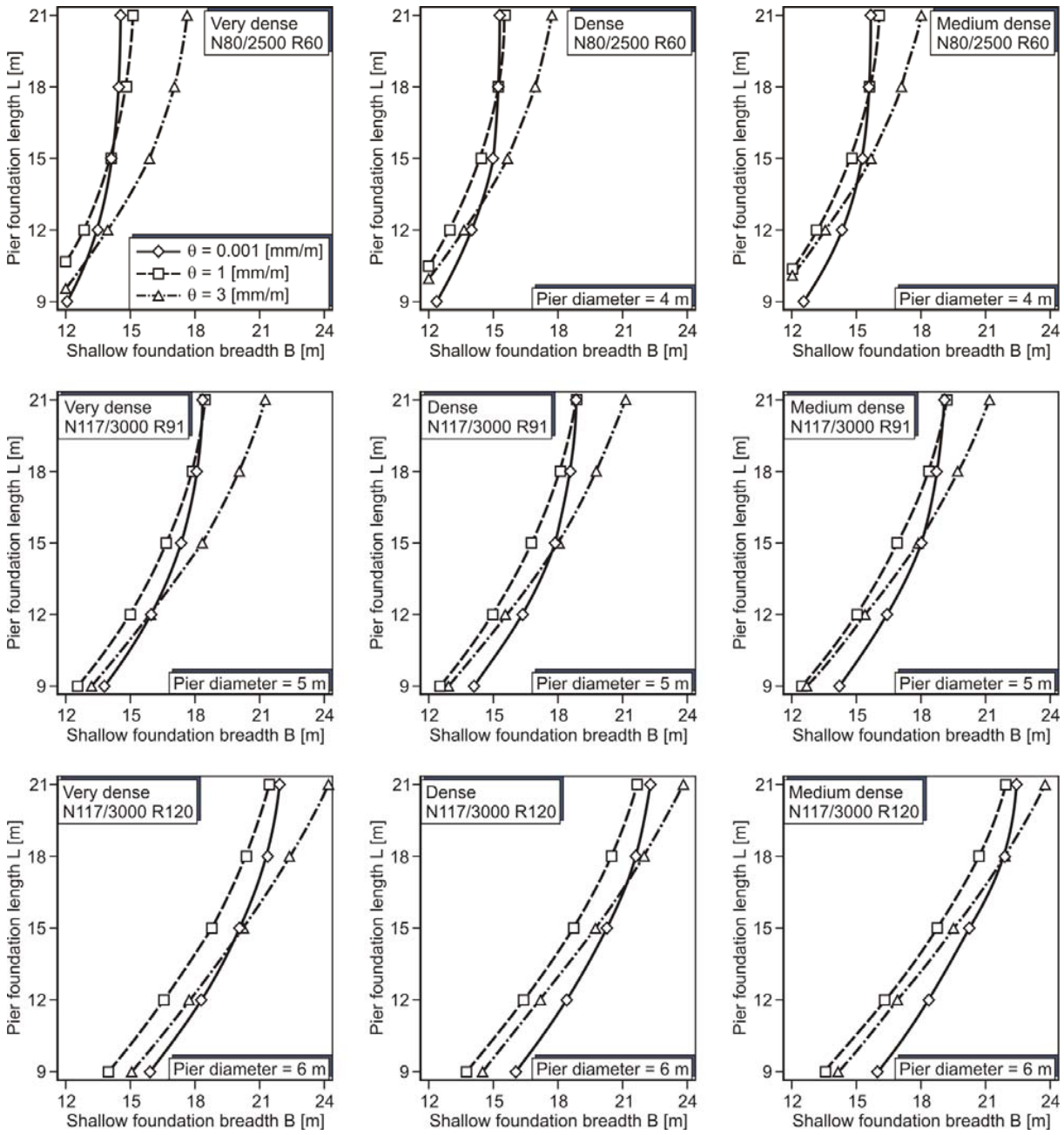

Fig. 8 Comparison of the pier and shallow foundations in terms of rotational stiffness

To reach the identical rotational stiffness of the shallow footings over the whole range of breadths analyzed, it was deemed suitable that the three predefined diameters (4, 5, 6 m) of pier foundation were allocated such that similar rotational stiffness of the shallow foundation was achieved.

It is evident that in all cases, the smaller head rotations θ = 0.001 and 1 mm/m are decisive to find a soil-pier system which satisfies all rotational stiffness requirements of the shallow foundation. This means that the SLS and FLS proofs might be critical for calculating the required length of a pier foundation, as shown in the relationship of the predefined head rotations between both foundation concepts.

Evidently, the variation of relative density from very dense to medium dense leads to an increment of the required pier length to obtain an identical rotational stiffness of the shallow foundation of OWT for the largest head rotation θ = 3 mm/m related to the ULS proof (extreme loads). Nevertheless, an opposite effect is produced due to a smaller increase of the rotational stiffness of the shallow foundations in comparison to the pier foundations for the smaller head rotations.

VI. Evaluation

Fig. 8 shows that for breadths of shallow foundation up to around 15 m, equivalent pier foundations with lengths of less than 12 m (depending on the chosen pier diameter) can be found. However, for enlarged foundation breadth, the required pier foundation length increases over-linear. For a shallow foundation breadth of 21 m, the required pier length is greater than 18 m for the maximum diameter of 6 m. Hence, the pier foundation could be a suitable solution for small wind turbines embedded in non-cohesive soil, but for large wind turbines the required foundation depth of the pier becomes quite large, which might make the application uneconomic. It is considered herein that the costs of an excavation pit necessary for the installation of the pier foundation also increase over-linear with depth. Nevertheless, using pier foundations for suitable cases makes a saving of concrete and reinforcement steel in comparison with the traditional foundation of OWT possible. According to [6], a reduction of concrete and steel which ranges from 50 to 75% and 40 to 55%, respectively, can be achieved. Due to the less reinforcement works; it also reduces the personal resources demands.

The pier foundation could also be a more convenient solution from environmental point of view, since it has a smaller footprint (dimension on ground view) than the shallow foundation. Furthermore, a predefined construction process adapted to mass production as established for the "P&H tensionless pier foundation" [6] can allow significant time and cost savings.

VII. Conclusion

A detailed evaluation of the load-bearing behavior of a pier foundation in comparison with the typical shallow foundation of OWT is carried out by a comprehensive parametric study under variation of the system boundary conditions for both soil-foundation systems. For such purpose, the HSsmall material law is applied to capture the non-linear behavior of the soil under virgin (monotonic) loading and also un- and reloading realistically. The rotational secant stiffness is considered as the reference parameter to obtain a general overview of the feasibility with respect to technical and economic issues to provide a comparison between both types of foundation. The following main conclusions can be drawn from the results of the numerical simulations:

- The application of the typical pier foundation appears to be acceptable for relatively small OWTs that are founded in stiff soil conditions such as very dense soils.
- The un- and reloading stiffness (translational and rotational) for different cyclic load spans can be described approximately by using the initial stiffness of the virgin (monotonic) load-deflection and moment-rotation curves.
- The comparative study demonstrates that there are certainly not equivalent systems between the two types of foundations for all load levels, simultaneously. This is caused by the fact that the stiffness behavior of both types of foundations is not similar.
- Based on the systematic comparison of the foundations presented, the SLS and FLS proofs seem to be decisive for the geotechnical design of pier foundations.

It is evident that further studies have to be conducted to consider all possible scenarios. The execution of field tests is highly desirable for more accurate calibration of future numerical models.

Acknowledgment

This study has been carried out within the ForWind joint research project "Ventus efficiens – Joint research for the efficiency of wind energy converters within the energy supply system," financially supported by the Ministry for Science and Culture in Lower Saxony, Germany. The authors thank the Ministry for Science and Culture in Lower Saxony for funding and all project partners for constructive cooperation.

References

[1] A. Quast, „Zur Baugrundsteifigkeit bei der gesamtdynamischen Berechnung von Windenergieanlagen", Mitteilung des Instituts für Grundbau, Bodenmechanik und Energiewasserbau der Universität Hannover, Heft 69, 2010.
[2] C.J. Warren-Codrington, "Geotechnical Considerations for Onshore Wind Turbines", University of Cape Town, November 2013, p. 205.
[3] DNV/Risø "Guidelines for the design of wind turbines", Second Edition, 2002.
[4] Deutsches Institut für Bautechnik, „Richtlinie für Windenergieanlagen. Einwirkungen und Standsicherheitsnachweise für Turm und Gründung", Schriften des DIBt, Heft 8, Fassung Oktober 2012.
[5] Deutsche Gesellschaft für Geotechnik (DGGT), „Empfehlungen des Arbeitskreises Baugrunddynamik", 1.Auflage, Dezember 2002.
[6] Earth Systems Southwest, "Patrick and Henderson (P&H) Foundations for Wind Turbine Support", Brochure, USA, 2009.
[7] Earth Systems Southwest, "Patrick & Henderson Tensionless pier", Presentation, USA, 2008.
[8] E. Ntambakwa, Y. Hao, C. Guzman, M. Rogers, "Geotechnical Design Considerations for Onshore Wind Turbine Shallow", Geotechnical and Structural Engineering Congress, Volume 2, 2016, pp. 1153-1165.
[9] J.A. Santos, A.G. Correia, "Reference threshold shear strain of soil and its application to obtain a unique strain-dependent shear modulus curve for soil", Proceedings of 15th International Conference on Soil Mechanics and Geotechnical Engineering, 2001, pp. 267-270.
[10] J. Ohde, „Zur Theorie der Druckverteilung im Baugrund", Der Bauingenieur 20, H. 33/34, pp. 451-459, 1939.
[11] K. Morgan, E. Ntambakwa, "Wind Turbine Foundation Behavior and Design Consideration", American Wind Energy Association Annual Conference and Exhibition, Houston, Texas, Volume 2, 2008, pp. 585-598.
[12] L.C. Reese, "Statement of Company Experience in Wind-Turbine Structures", report, 2008.
[13] M. Achmus, K. Thieken, J.E. Saathoff, M. Terceros, J. Albiker, "Un- and reloading stiffness of monopile foundations in sand", Applied Ocean Research, Volume 84, pp. 62-73. March 2019.
[14] M. Achmus, "Soil Investigation and Foundation for Wind Turbines", HdT-Conference, July 2013.
[15] Nordex, "Turbine and Tower Technical Data", February 2012.
[16] R.B.J. Brinkgreve, S. Kumarswamy, and W.M. Swolfs, "PLAXIS 3D Manual", 2016.
[17] T. Benz, "Small Strain Stiffness of Soils and its Numerical Consequences", Ph.D. thesis, University of Stuttgart, Stuttgart, Germany, 2007, 193 pp.
[18] T. Schanz, „Zur Modellierung des mechanischen Verhaltens von Reibungsmaterialien", University of Stuttgart, Habilitation, 1998.
[19] United State Patent "Tensionless pier foundation, patent number 5586417", Inventors A. P. Henderson & M. B. Patrick, 1996.